

Observation of Acoustic Umklapp Phonons in Water-Stabilized DNA by Neutron Scattering

H. Grimm and H. Stiller

Kernforschungsanlage Jülich, D-5170 Jülich, West Germany

C. F. Majkrzak

Brookhaven National Laboratory, Upton, New York 11973

A. Rupprecht

Arrhenius Laboratory, University of Stockholm, S-106 91 Stockholm, Sweden

and

U. Dahlborg

Institute of Reactor Physics, Royal Institute of Technology, S-100 44 Stockholm, Sweden

(Received 16 June 1987)

We have investigated static and dynamic properties of wet-spun DNA fibers in their *C*, *A*, and *B* conformations using thermal-neutron scattering. Overdamped and underdamped longitudinal acoustic umklapp phonons are observed in the vicinity of a hydration-dependent two-dimensional sheet of diffuse scattering perpendicular to the helix axis. A quantitative analysis of this mode is presented for the *B*-DNA sample in terms of a harmonic one-dimensional liquid, i.e., taking into account all orders of fluctuations. The resulting effective dispersion does not extrapolate to zero frequency at the position of the sheet.

PACS numbers: 87.15.-v, 25.40.Fq, 43.20.+g

The important role of water in stabilizing the structures of DNA has been recognized by the variation of x-ray patterns with the humidity of the fiber.¹ Many details have been investigated for a better understanding of this subtle interaction,² i.e., by studies on hydration sites and binding energies,³ on spine formation,⁴ and on the influence of counterions,⁵ as well as by elucidating computer simulations.⁶

Thermal-neutron scattering can be expected to contribute significantly to the picture of this hull of water because of the suitable cross sections for hydrogen and deuterium and because this scattering yields simultaneously information about space and time correlations. The drawback of the large enough sample volume was overcome by the development and perfection of the wet-spinning method.⁷ By folding the resulting strip of well-oriented DNA (≈ 0.5 degrees) one may achieve sample volumes up to 1 cm³. In the first neutron-scattering experiments with such samples,⁸ a broad peak at $Q_{\parallel} \approx 1.9 \text{ \AA}^{-1}$ was detected, which was absent for dry DNA.

Two questions—intimately related to this finding—had to remain unanswered because of flux, instrumental, and sample limitations: (i) How is this broad peak related to the usual “Bragg reflections” representing the DNA molecule only? (ii) What excitations are connected with this peak?

Aiming at these questions, we have reinvestigated the semicrystalline sample used earlier⁸ (*C* conformation, 9.3 residues in a pitch of 31 Å) and, in addition, two new samples of higher crystallinity (*A* and *B* conformations, 11 and 10 residues in pitches of 28.2 and 33.8 Å, respec-

tively; compared to the Watson-Crick *B* helix the average angle between the helix axis and the base pairs is about 70 degrees for the *A* conformation and the base pair center is shifted outwards²). Before being sealed into aluminum containers, the samples were equilibrated to 75% relative humidity over saturated NaClO₃ solution in D₂O or H₂O. The measurements were performed on three-axis spectrometers in Jülich (reactor DIDO) and at Brookhaven National Laboratory (High Flux Beam Reactor). Pyrolytic-graphite crystals and an average horizontal collimation of 40' were used to select the incident and scattered neutrons. An initial energy of about 3.55 THz in conjunction with an aligned pyrolytic-graphite filter was chosen to avoid contamination of the beam from higher-order scattered neutrons. The illuminated sample volume was about 40×40×0.7 mm³.

The exploration of the dynamics of these three samples was preceded by an investigation of the elastic neutron scattering. Besides the corroboration of the x-ray characterization and the inspection of the quality of the overall helix alignment, these measurements shed light on the origin of the broad peak mentioned above. Figure 1 presents some elastic scans [energy resolution 0.23 THz full width half maximum (FWHM)] in a region of momentum transfers \mathbf{Q} corresponding to the first maximum in the structure factor $S(Q)$ of D₂O with \mathbf{Q} oriented parallel to the helix axis ($\equiv Q_{\parallel}$) for the three D₂O-hydrated conformations of DNA. Comparing bulk D₂O with the semicrystalline *C*-DNA, one recognizes in both cases a constructive interference at $Q \approx 1.92 \text{ \AA}^{-1}$. For bulk D₂O this peak is known to result from interfer-

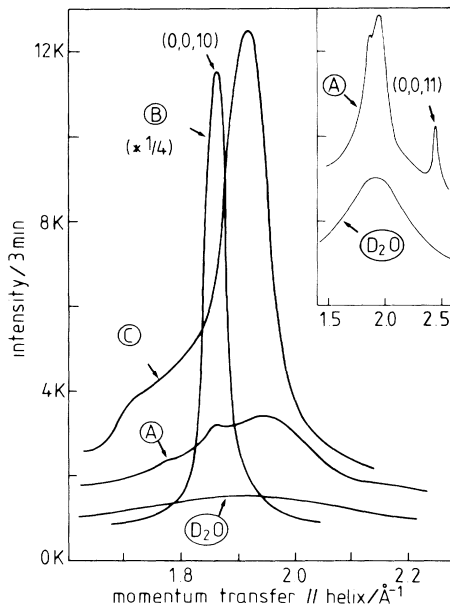


FIG. 1. Elastic scans (within energy resolution of 0.23-THz FWHM) along the helix axis in the region of the first peak in the structure factor of water ($\approx 1.92 \text{ \AA}^{-1}$; see curve for bulk D_2O). The results are given as lines because of the good statistics. The intensities are directly comparable since sample volume and experimental conditions were similar for all four scans. The symbols *A, B, C* correspond to the conformations of DNA (hydrated to 75% relative humidity by D_2O).

ence between O-O and O-D of next-neighbor molecules.⁹ The same origin can be supposed for the broad peak observed for C-DNA not only because of its sensitivity to humidity variation but also—and primarily—because of its incommensurability with $c^* = 2\pi/c = 0.203 \text{ \AA}^{-1}$ for

C-DNA.¹ The broad C-DNA peak represents actually a scan through a disklike distribution of scattering intensity with a diameter of 0.75 to 0.8 \AA^{-1} and a thickness of $\approx 0.09 \text{ \AA}^{-1}$ (FWHM). This scattering may be interpreted as the first sheet of scattering from a linear chain of some objects described by the geometric series of the average next-neighbor phase factor $\exp[iQ_{\parallel}c - Q_{\parallel}^2 u^2/2]$,

$$S(Q_{\parallel}) = \frac{\sinh(Q_{\parallel}^2 u^2/2)}{\cosh(Q_{\parallel}^2 u^2/2) - \cos(Q_{\parallel}c)} \quad (1)$$

The intensity within these sheets at $Q_{\parallel}c \approx 2n\pi$ is modulated by the form factor of this object. From the position and thickness of the disklike scattering follow a next-neighbor distance $c = 3.29 \text{ \AA}$ and its fluctuation $u^2 = 0.08 \text{ \AA}^2$.

The peak is still visible for A-DNA but slightly shifted to a next-neighbor distance of 3.22 \AA . In addition two new—more sharply defined—periodicities occur, i.e., the (0,0,11) reflection at 2.46 \AA^{-1} , being typical for A-DNA, together with an indication of the (0,0,10) reflection at $Q_0 = 1.86 \text{ \AA}^{-1}$, signaling some portion of B-DNA in coexistence. A monotonic change into the peak for the C-DNA sample was observed by increasing the humidity of a similar A-DNA sample (better surface exposure in order to allow for variation of humidity during the measurement). Finally, for the highly crystalline B-DNA, the “disk” is locked in with the skeleton reflections. Again, the disklike shape—now with a diameter of 0.57 \AA^{-1} —is recognizable in scans perpendicular to the helix axis. The skeleton reflections are superimposed. Actually, the (0,0,10) reflection is rather weak and accounts for less than 10% of the scattering shown in Fig. 1. The parameters of Eq. (1) are $c = 3.38 \text{ \AA}$ and $u^2 = 0.043 \text{ \AA}^2$ for B-DNA.

The emerging picture is that of a mutual stabilization

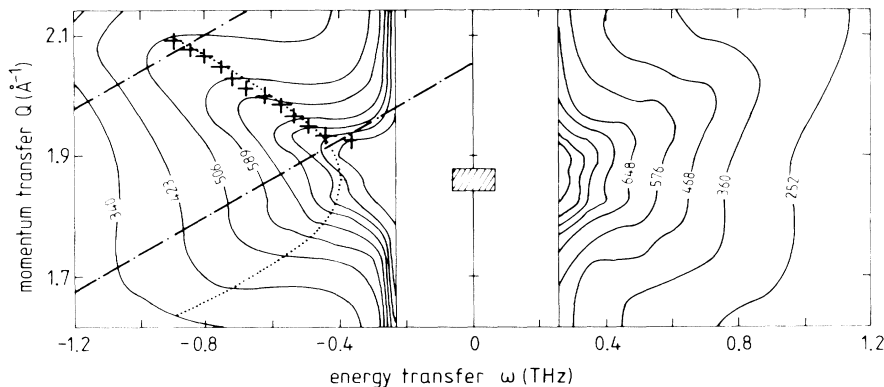


FIG. 2. Contour map of the scattered intensity from B-DNA in the (Q_{\parallel}, ω) plane. The figures at the equidistant contour lines denote counts per about two minutes. Position and width of the peak shown in Fig. 1 is indicated by the shaded area. The dashed-dotted lines correspond to the paths of the first and last scans displayed in Fig. 3. The crosses mark the fitted peak positions of those and similar scans. The apparent deviation of the cross for the lowest frequency is very likely due to the fact that the resolution ellipsoid “picks up” already some intensity from the (1,0,10) reflection. The dotted line corresponds to Eq. (3).

and final lock-in of two incommensurate structures, the DNA skeleton and a more or less linearly ordered water. Note that two periodic structures may interact by common wave vectors only. In this respect, the malleable next-neighbor distance of water molecules seems to be advantageous since it provides a broad response around 2 \AA^{-1} .

Low-frequency excitations have been identified for *C*- and *A*-DNA which are uniquely related to the helix axis and associated with the peaks at 1.92 \AA^{-1} and 1.95 \AA^{-1} , respectively. The less overdamped spectra for *C*-DNA suggest their interpretation as longitudinal acoustic phonons. A full account of these observations together with the statics of DNA as "seen" by neutrons and details of the sample preparation will be published elsewhere. Underdamped acoustic excitations were observed for the *B*-DNA sample as shown by the contour map in the (Q_{\parallel}, ω) plane (Fig. 2). The asymmetry with respect to $Q_0 = 1.86 \text{ \AA}^{-1}$ vanishes within statistics if the intensities are divided by Q_{\parallel}^2 . This is compatible with the eigenvector for an acoustic mode. The longitudinal character is demonstrated by the visibility of the excitation for \mathbf{Q} parallel to the helix axis only.

The sample shows aspects of both a three-dimensional solid and a one-dimensional liquid. In addition to strong damping of the excitations, one observes a weak second diffuse sheet at $Q_{\parallel} \approx 3.75 \text{ \AA}^{-1}$ which is more than three times broader than the first one [a factor of 4 is implied by Eq. (1)]. Therefore, we have based the analysis on the 1D liquid picture.¹⁰ Because of the strong fluctuations for one dimension *all multiphonon contributions* have to be considered. This leads to the somewhat

unusual form of the scattering function¹¹

$$S(\Delta Q, \omega) = L(\Delta Q + \omega/v)L(\Delta Q - \omega v), \quad (2)$$

with $\Delta Q = Q_{\parallel} - Q_0$ and the sound velocity v being assumed constant. The function $L(x)$ may be approximated by a Lorentzian with FWHM $2\Gamma = (c^*u)^2/c$ for small arguments. As expected for a liquid there is no truly elastic scattering. The form of Eq. (2) suggests that we extract information about the two parameters v and Γ from constant-*velocity* scans rather than from const- \mathbf{Q} scans. Those scans are indicated in Fig. 2 by the dash-dotted lines together with the obtained peak positions. The corresponding intensity variation is compared to the measurement in Fig. 3.

In agreement with the *Ansatz* we obtain within the fitted range and statistics a constant sound velocity $v = 1.85 \pm 0.05 \text{ km/sec}$ and an approximately constant damping $\Gamma = 0.12 \pm 0.01 \text{ \AA}^{-1}$, the latter being compatible also with the intensity variation. Compared with the elastic-scattering data (Fig. 1), there remain two inconsistencies: (i) The mean fluctuations u^2 corresponding to this value of Γ are larger than expected for the harmonic chain by a factor of 3.5 to 5.5 (for perfect to no ω resolution, respectively) and (ii) the linear extrapolation to zero frequency deviates by about 0.07 \AA^{-1} (≈ 1.6 FWHM of the elastic scan) from Q_0 . In fact, velocities as high as 6 km/sec would be necessary to "hit" Q_0 by extrapolation. A satisfactory description of the fitted peak positions is achieved by allowing for an effective hyperbolic dispersion relation

$$\omega^2 = \omega_0^2 + v^2(\Delta Q)^2 \quad (3)$$

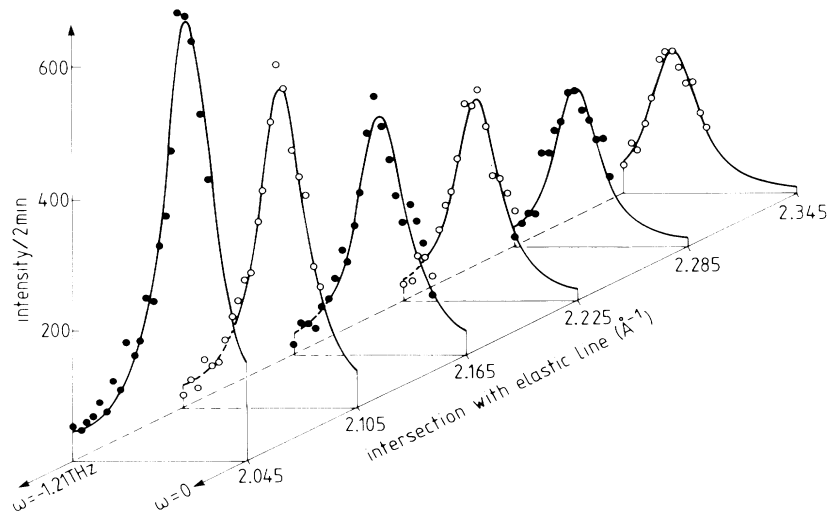


FIG. 3. Series of constant-velocity scans for *B*-DNA in the (Q_{\parallel}, ω) plane as indicated in Fig. 2. The chosen velocity for the scan direction is 2.026 km/sec or $3.224 \text{ THz/\AA}^{-1}$. The scans intersect the elastic line at the indicated values for Q_{\parallel} . The intensities correspond to the difference between the orientation of the momentum transfer parallel and perpendicular to the helix axis. The solid lines represent individual Lorentzians folded with the resolution of the spectrometer.

with $\omega_0=0.4$ THz and a sound velocity being now increased to $v=2.18$ km/sec (dotted line in Fig. 2). Our value of v agrees well with the Brillouin spectra obtained from a similar sample¹² after a careful study of the effect of laser heating.¹³

The finite value of ω_0 and the large value of Γ might be indicative of the influence of an optic mode. However, the dynamical structure factor is zero at \mathbf{Q}_0 for the two modes which are likely to have a low restoring force, i.e., the antiphase motions of the two strands of the helix or of neighboring chains. In addition, there is no apparent nonmonotonic variation of the scattered intensity indicating the crossover with an optic mode.

A possible "explanation" of ω_0 by the spread of the helix direction seems also not likely because of the quasi one-dimensional features of $S(\mathbf{Q},\omega)$. This was verified by ω scans at \mathbf{Q} slightly off from the average helix direction. No apparent shift of the peak position with Q_\perp was observed but rather a reduction of the peak intensity, which is mainly attributed to the limited lateral extent of the "elastic disk".

Thus one may conclude that the analysis presented so far suggests the consideration of 1D chains which incorporate in addition the effect of disorder. Disorder may enter via a fluctuation of forces and masses^{14,15} (random sequence of nucleic acids) or slipping over local potential barriers^{10,16} (e.g., as a result of weak lateral interactions as indicated by the weak lateral Bragg reflections on top of the disk). Both types of disorder might be indicated by ω_0 and Γ . Temperature- and humidity-dependent measurements may help to reveal their relative importance.

We would like to thank V. J. Emery, J. D. Axe, and H. J. Mikeska for helpful discussions. Two of us (H.G. and H.S.) thank the staff at Brookhaven National Laboratory for hospitality and assistance. The work at Brookhaven National Laboratory was supported by the

Division of Material Sciences, U.S. Department of Energy under Contract No. DE-AC02-76CH00016.

¹R. E. Franklin and R. G. Gosling, *Acta Crystallogr.* **6**, 673 (1953).

²An updated key to the related literature may be found in *Structure and Dynamics: Nucleic Acids and Proteins*, edited by E. Clementi and R. H. Sarma (Adenine, New York, 1982).

³M. Falk, K. A. Hartmann, Jr., and R. C. Lord, *J. Am. Chem. Soc.* **84**, 3843 (1962), and **85**, 387 (1963).

⁴R. E. Dickerson, *Sci. Am.* **249**, No. 6, 94 (1983); M. L. Kopka, A. V. Fratini, H. R. Drew, and R. E. Dickerson, *J. Mol. Biol.* **163**, 129 (1983).

⁵P. J. Cooper and L. D. Hamilton, *J. Mol. Biol.* **16**, 562 (1966).

⁶E. Clementi and G. Corongiu, *Chem. Phys. Lett.* **60**, 175 (1979), and *Biopolymers* **18**, 2432 (1979).

⁷A. Rupprecht, *Biotechnol. Bioeng.* **94**, 99 (1970), and *Acta Chem. Scand. Ser. B* **33**, 779 (1979).

⁸U. Dahlborg and A. Rupprecht, *Biopolymers* **10**, 849 (1971).

⁹See, e.g., *Water—A Comprehensive Treatise*, edited by F. Franks (Plenum, New York, London, 1972), Vol. 1, p. 344.

¹⁰J. D. Axe, in *Ordering in Strongly Fluctuating Condensed Matter Systems*, edited by T. Riste (Plenum, New York, 1980), p. 399; V. J. Emery and J. D. Axe, *Phys. Rev. Lett.* **40**, 1507 (1978).

¹¹H. J. Mikeska, *Solid State Commun.* **13**, 73 (1973).

¹²C. Demarco, S. M. Lindsay, M. Pokorny, J. Powell, and A. Rupprecht, *Biopolymers* **24**, 2035 (1985).

¹³M. B. Hakim, S. M. Lindsay, and J. Powell, *Biopolymers* **23**, 1185 (1984).

¹⁴S. Takeno and M. Goda, *Prog. Theor. Phys.* **47**, 790 (1972).

¹⁵K. Kim and M. Nelkin, *Phys. Rev. B* **7**, 2762 (1973).

¹⁶J. A. Krumhansl and J. R. Schrieffer, *Phys. Rev. B* **11**, 3535 (1975).